

Electronic Supplementary Information (ESI)

Stimuli Responsive PEGylated Bismuth Selenide Hollow Nanocapsules for Fluorescence/CT imaging and Light-Driven Multimodal Tumor Therapy

Lihong Sun ^{a, b}, Qian Li ^{a, b}, Lei Zhang ^c, Huihui Chai ^{a, b}, Ling Yu ^{a, b}, Zhigang Xu ^{a, b},
Yuejun Kang ^{a, b}, Peng Xue ^{a, b*}

^a Key Laboratory of Luminescent and Real-Time Analytical Chemistry (Southwest University), Ministry of Education, School of Materials and Energy, Southwest University, Chongqing 400715, China.

^b Chongqing Engineering Research Center for Micro-Nano Biomedical Materials and Devices, Southwest University, Chongqing 400715, China.

^c Institute of Sericulture and System Biology, Southwest University, Chongqing 400716, China.

Corresponding author:

Email: xuepeng@swu.edu.cn (P. Xue)

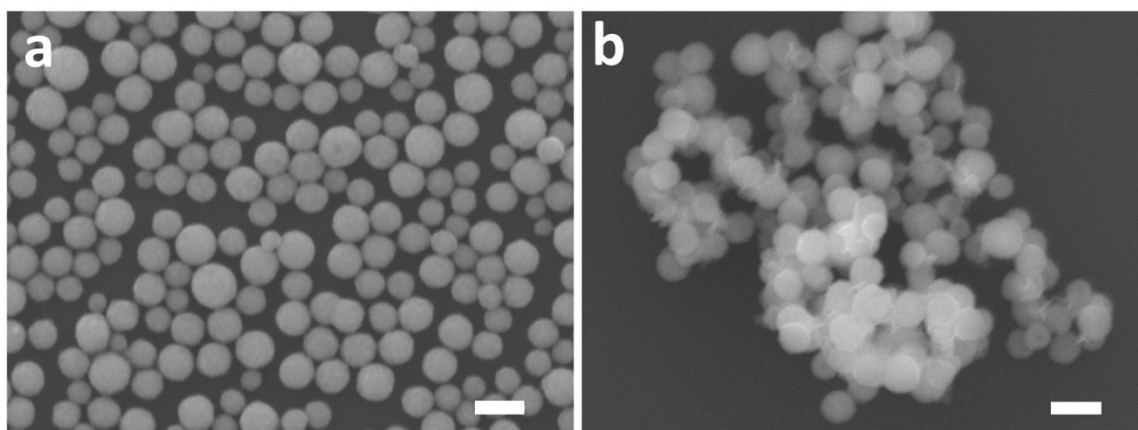


Fig. S1 FESEM images of (a) Bi_2O_3 NPs and (b) Bi_2Se_3 NCs (scale bars: 200 nm).

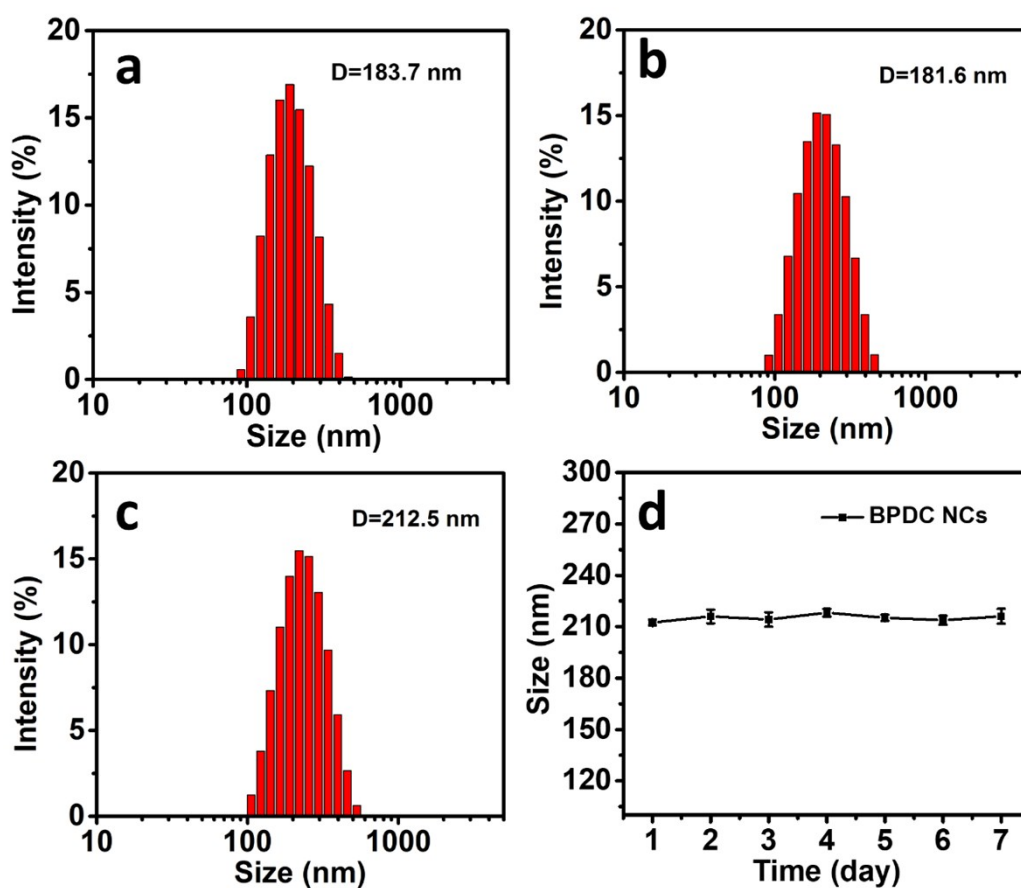


Fig. S2 Size distribution of (a) Bi_2O_3 NPs, (b) Bi_2Se_3 NCs and (c) Bi_2Se_3 @PEG NCs measured by DLS; (d) Hydrodynamic size variation of BPDC NCs under aqueous condition for seven days.

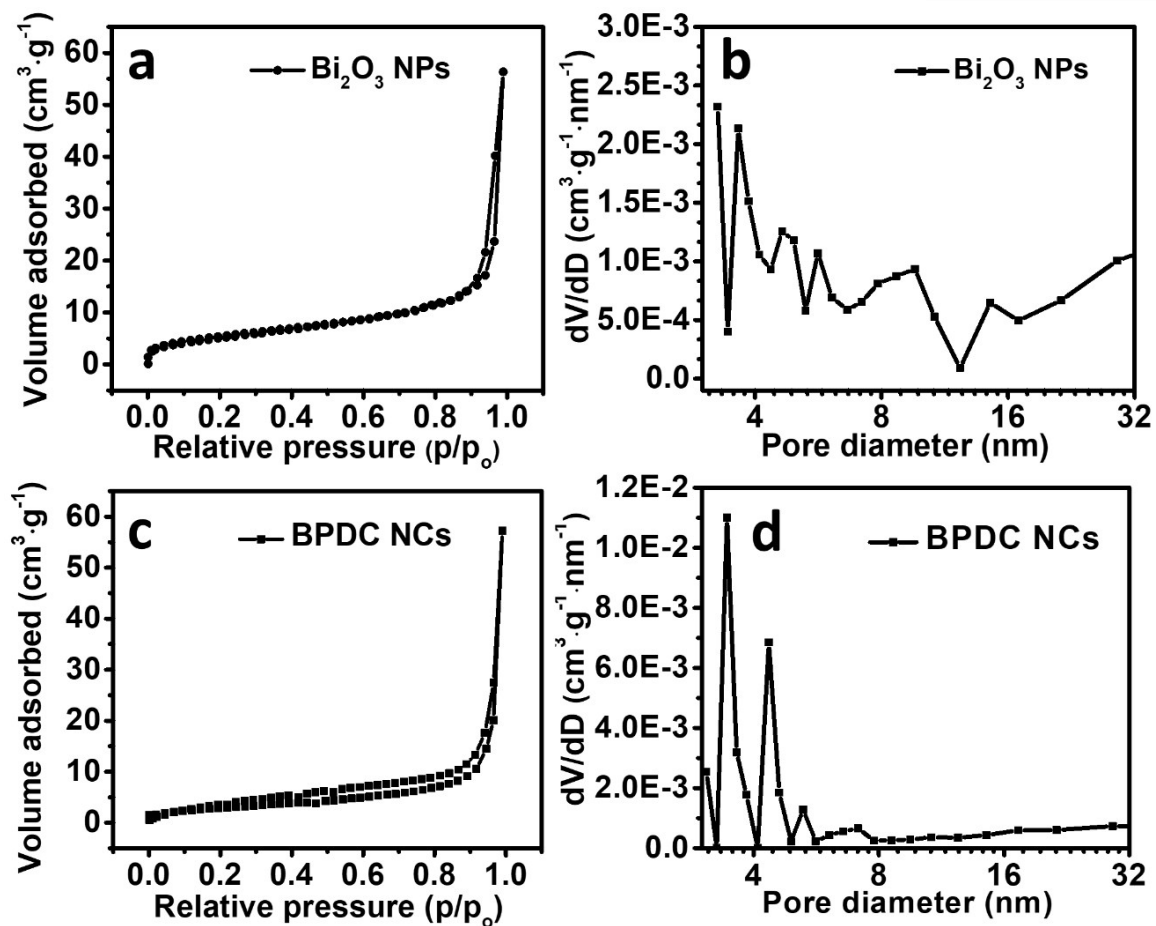


Fig. S3 (a) N₂ adsorption–desorption isotherm and (b) the corresponding pore size distribution of the Bi₂O₃ NPs; (c) N₂ adsorption–desorption isotherm and (d) the corresponding pore size distribution of the BPDC NCs.

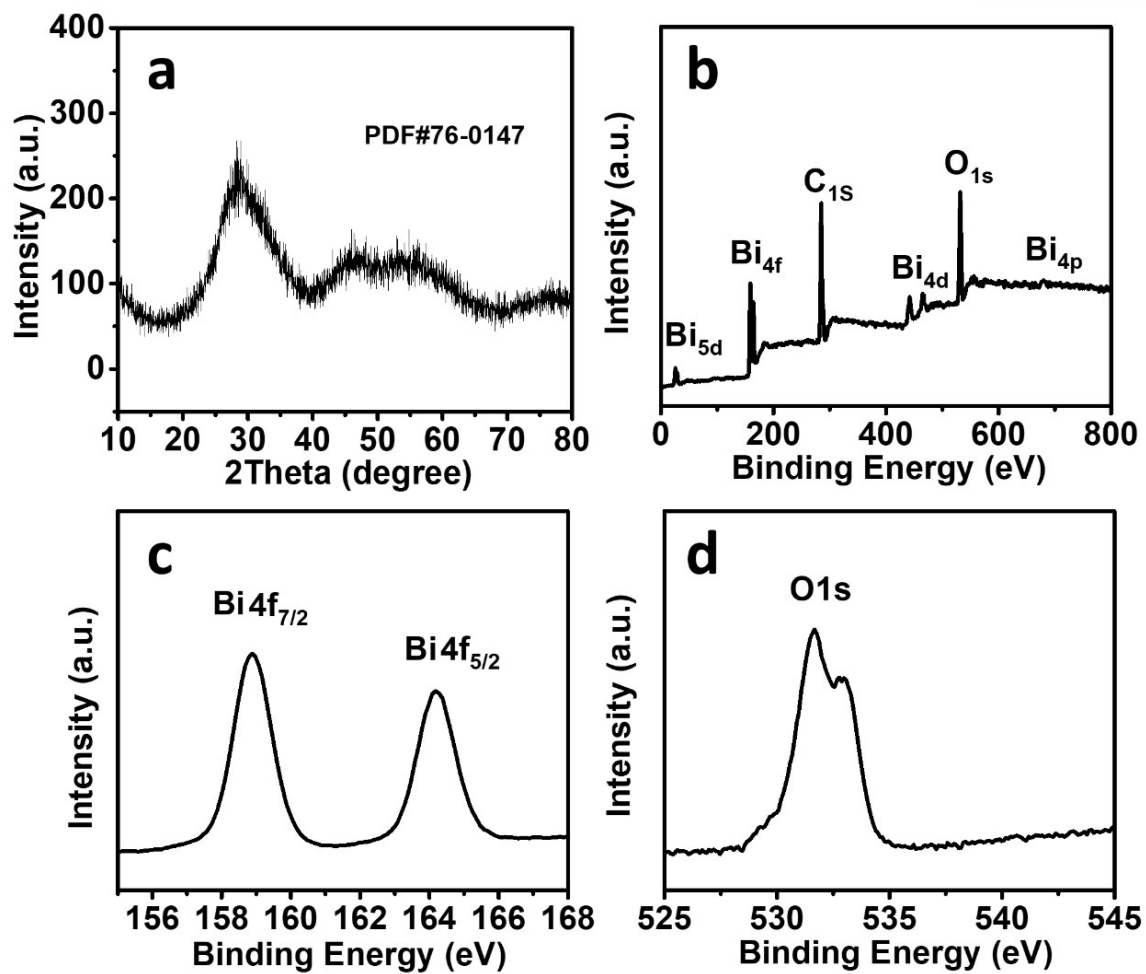


Fig. S4 (a) XRD pattern of Bi₂O₃ NPs; (b-d) XPS characterization of Bi₂O₃ NPs: (b) the survey of full spectrum and core level spectrum of (c) Bi4f (d) O1s.

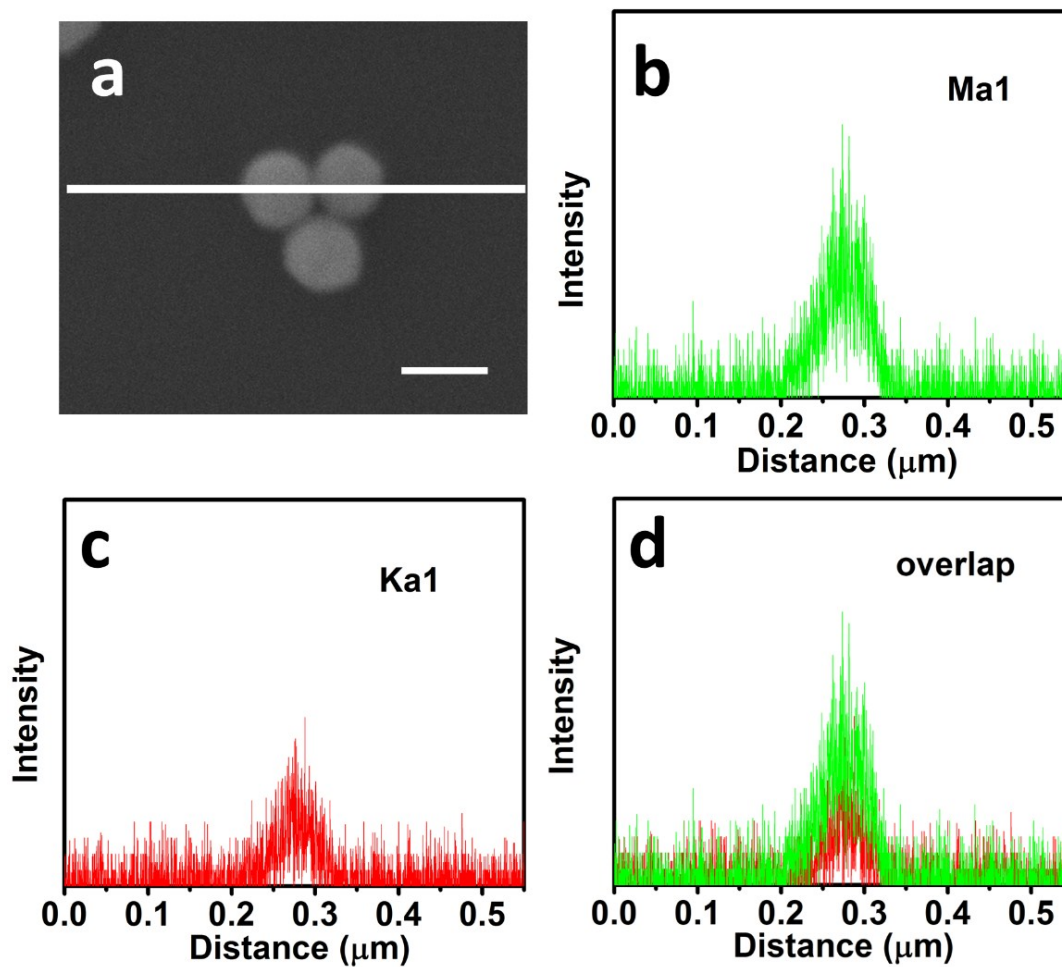


Fig. S5 (a) Typical TEM image of Bi_2O_3 NPs (scale bar: 100 nm); (b-d) linear scanning results of the cross-section of individual Bi_2O_3 NP based on EDS analysis.

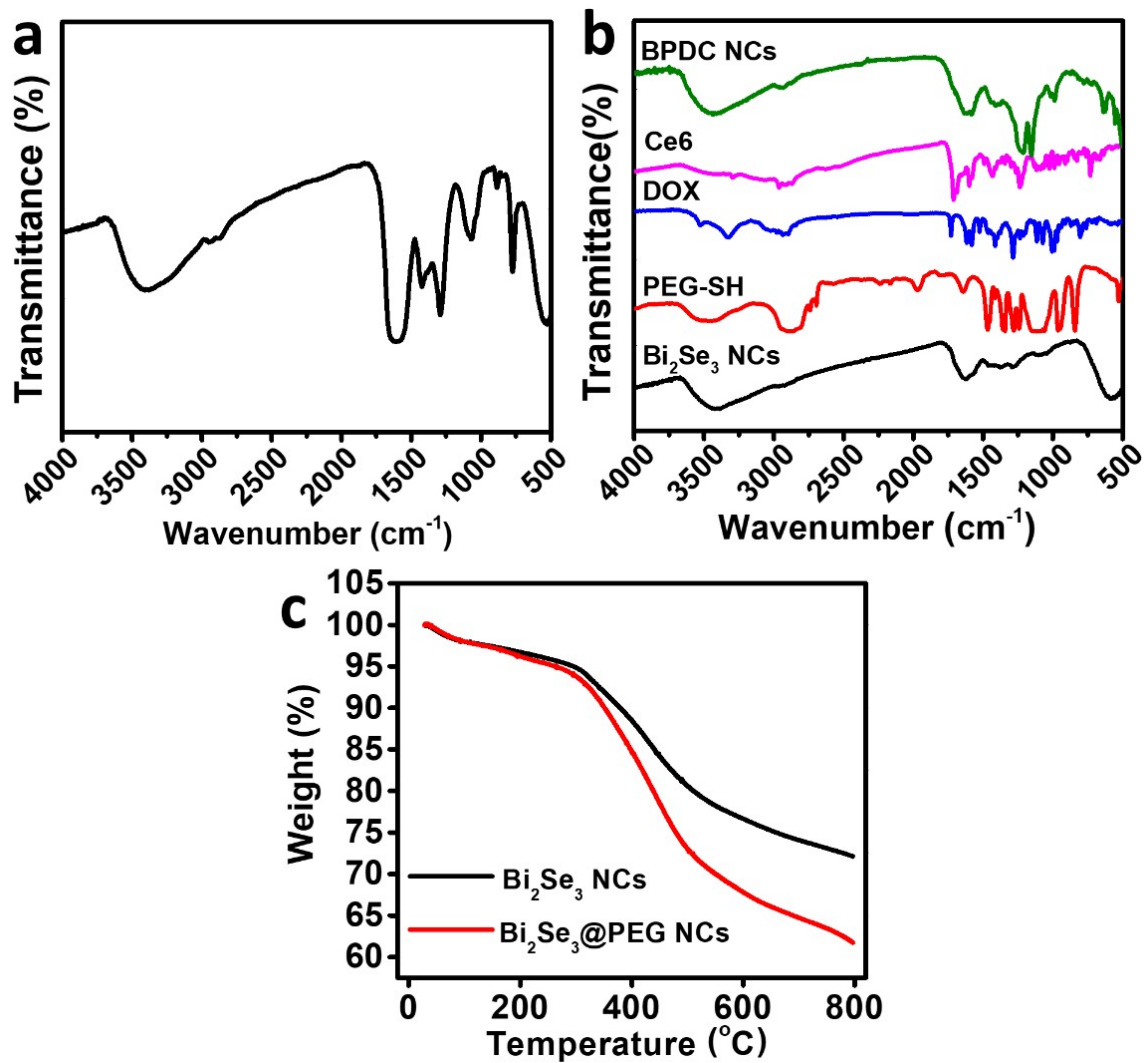


Fig. S6 FTIR spectra of (a) Bi_2O_3 NPs and (b) Bi_2Se_3 NCs, PEG-SH, DOX, Ce6, BPDC NCs; (c) TGA curves of Bi_2Se_3 NCs and Bi_2Se_3 @PEG NCs.

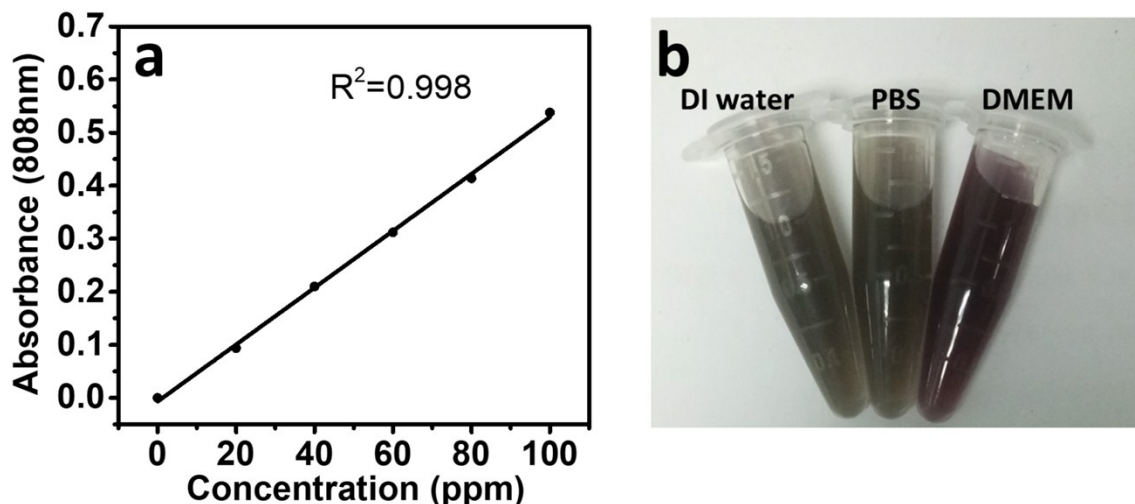


Fig. S7 (a) Fitting curve of the NIR absorbance of BPDC NCs at 808 nm as the function of sample concentration ranging from 0 to 100 ppm; (b) image of BPDC NCs dispersed in DI water, 1×PBS and DMEM culture medium.

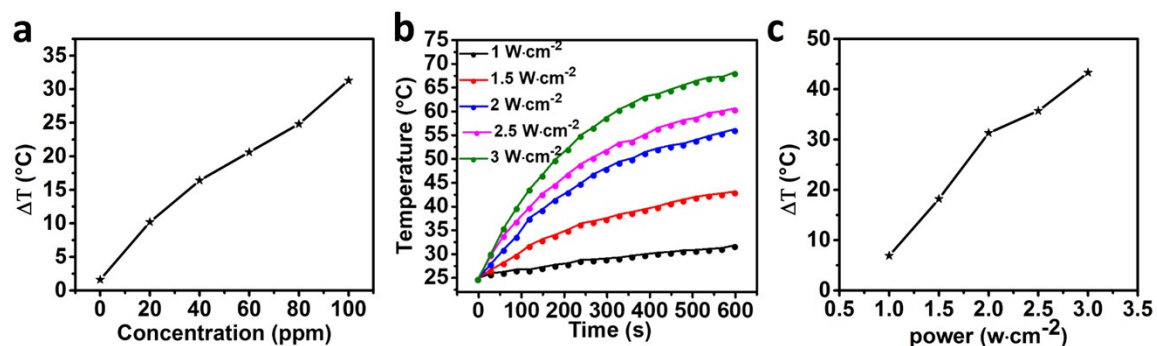


Fig. S8 (a) Temperature variation of BPDC NCs after being irradiated by an NIR laser (808 nm, $2 \text{ W}\cdot\text{cm}^{-2}$) for 10 min versus the agent concentrations ranging from 0 to 100 ppm; (b) temperature elevation of the BPDC NC dispersion (100 ppm) under NIR laser irradiation for 10 min at various output power intensity (1 to $3 \text{ W}\cdot\text{cm}^{-2}$); (c) temperature variation in the BPDC NCs (100 ppm) after NIR laser irradiation for 10 min versus the output power intensity (1 to $3 \text{ W}\cdot\text{cm}^{-2}$).

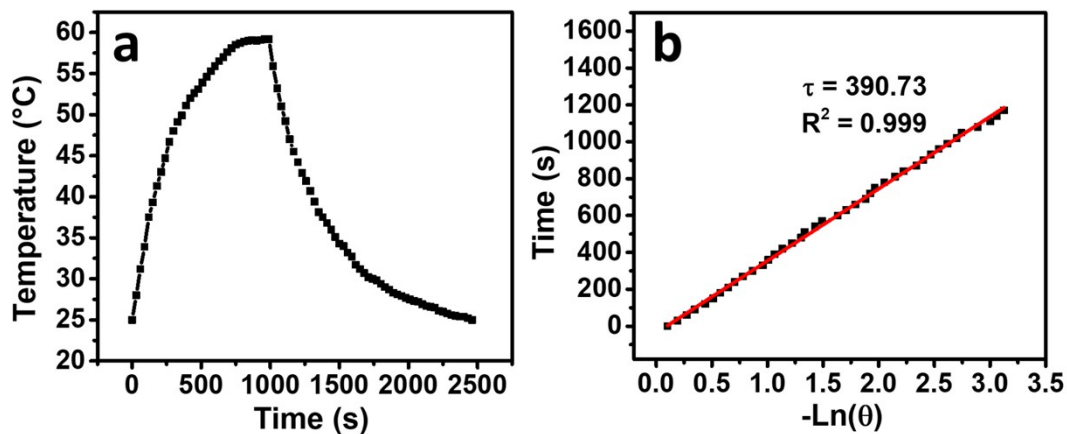


Fig. S9 (a) Heating and cooling curves of BPDC NC suspension (1mL, 100 $\mu\text{g}\cdot\text{mL}^{-1}$) subject to NIR laser irradiation; (b) diagram of the time versus $-\ln(\theta)$ derived from the cooling stage in (a).

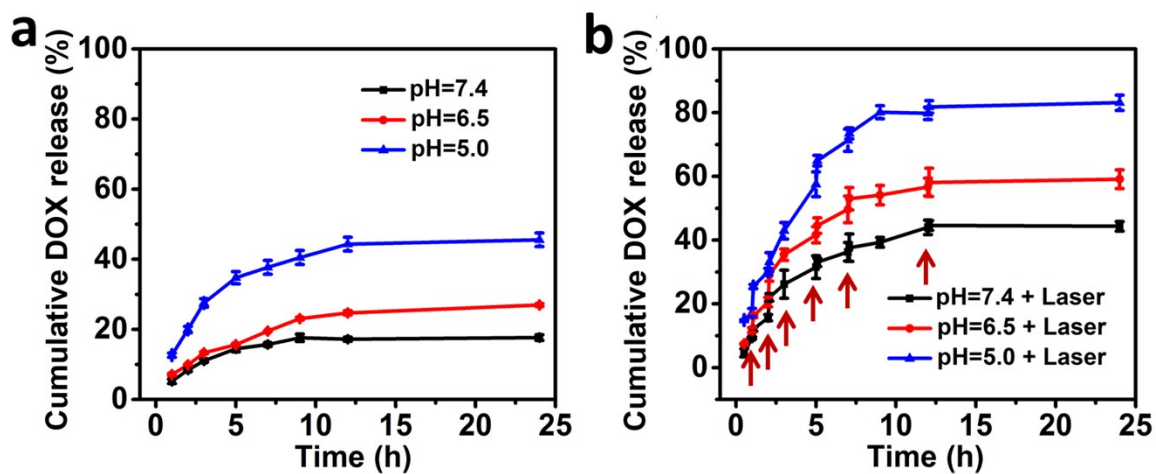


Fig. S10 Release kinetics of DOX from BPDC NCs under pH 5.0, 6.5 and 7.4 (a) without laser irradiation or (b) with periodic laser irradiation (laser on for 5 min per cycle).

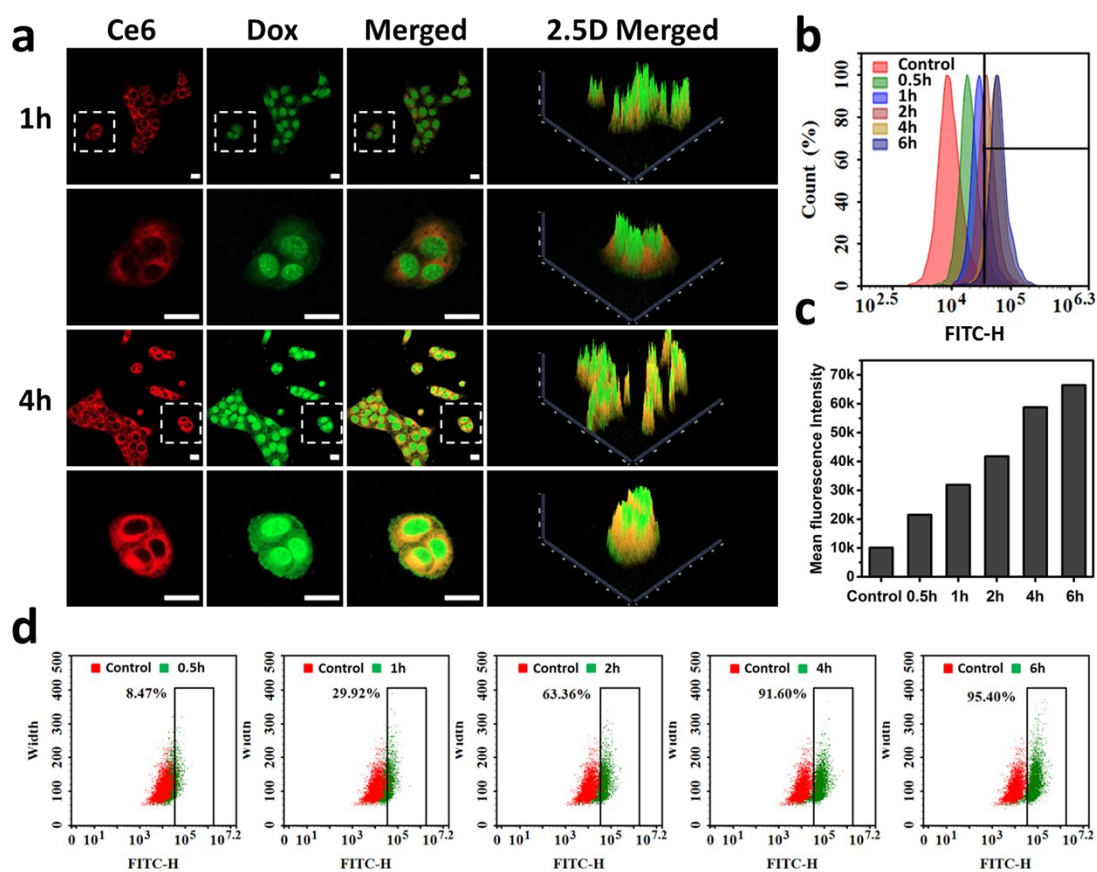


Fig. S11 Characterizations of cellular uptake of DOX mediated by BPDC NCs. (a) confocal microscopy: fluorescence images of 4T1 cells being treated by BPDC NCs for 1 h or 4 h (scale bars: 20 μ m). The fluorescence signal of DOX and Ce6 are displayed in green and red color, respectively (scale bars: 20 μ m. Images of 2nd and 4th row are the magnification of dashed box enclosed area in 1st and 3rd row, respectively); (b) flow cytometry to analyze the cellular uptake of DOX mediated by BPDC NCs in 4T1 cells after various incubation periods; (c) mean intensity of DOX fluorescence emission from cells corresponding to (b); (d) flow cytometry dot plots of 4T1 cells after being treated by BPDC NCs for different periods.

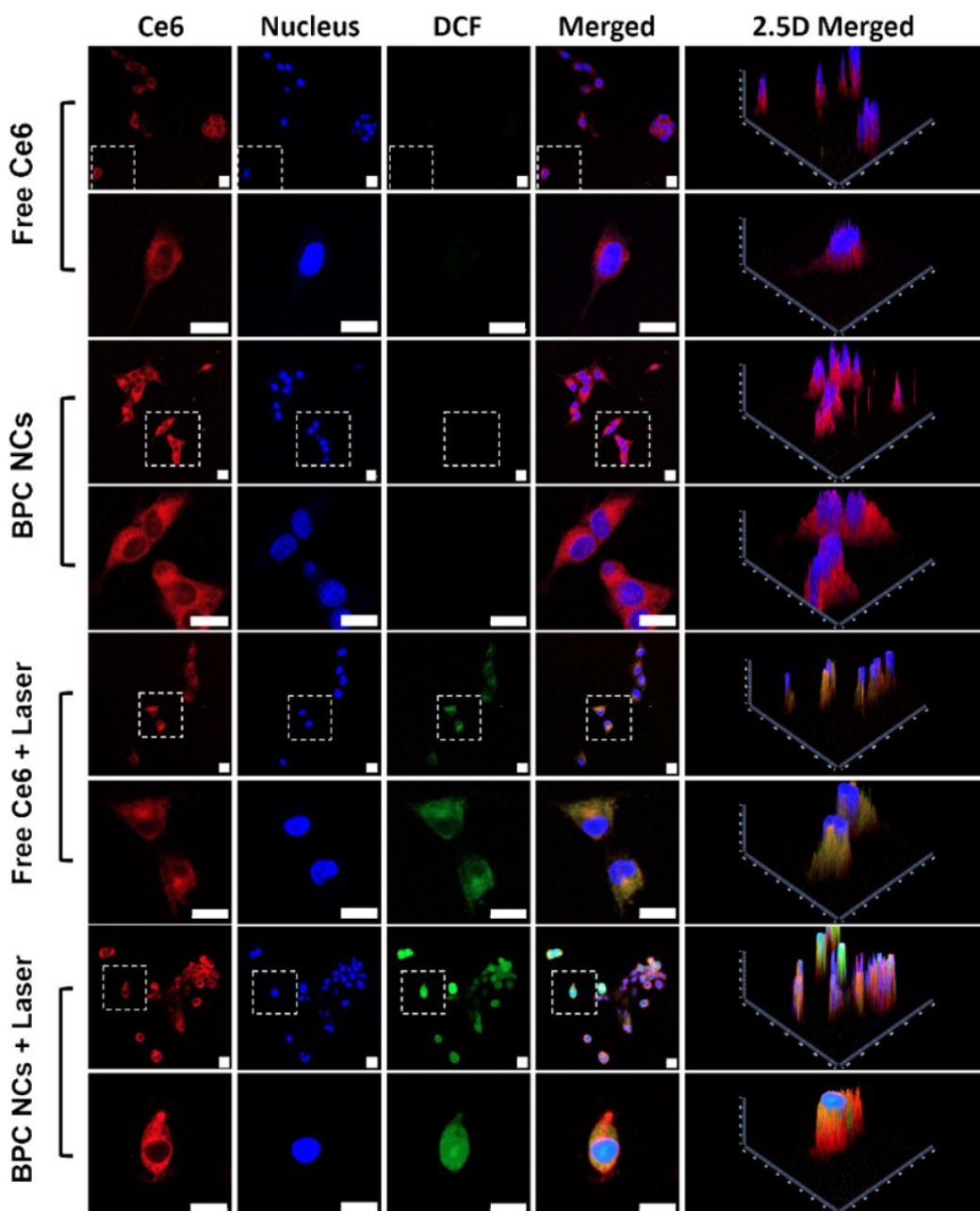


Fig. S12 Characterization of intracellular ROS generation through DCFH-DA probe: confocal fluorescence images of 4T1 cells being treated with free Ce6 or BPC NCs subject to 660 nm laser irradiation where applicable (scale bars: 20 μm). Images in 2nd, 4th, 6th and 8th rows display the magnified areas enclosed in dashed box in 1st, 3rd, 5th and 7th rows, respectively.

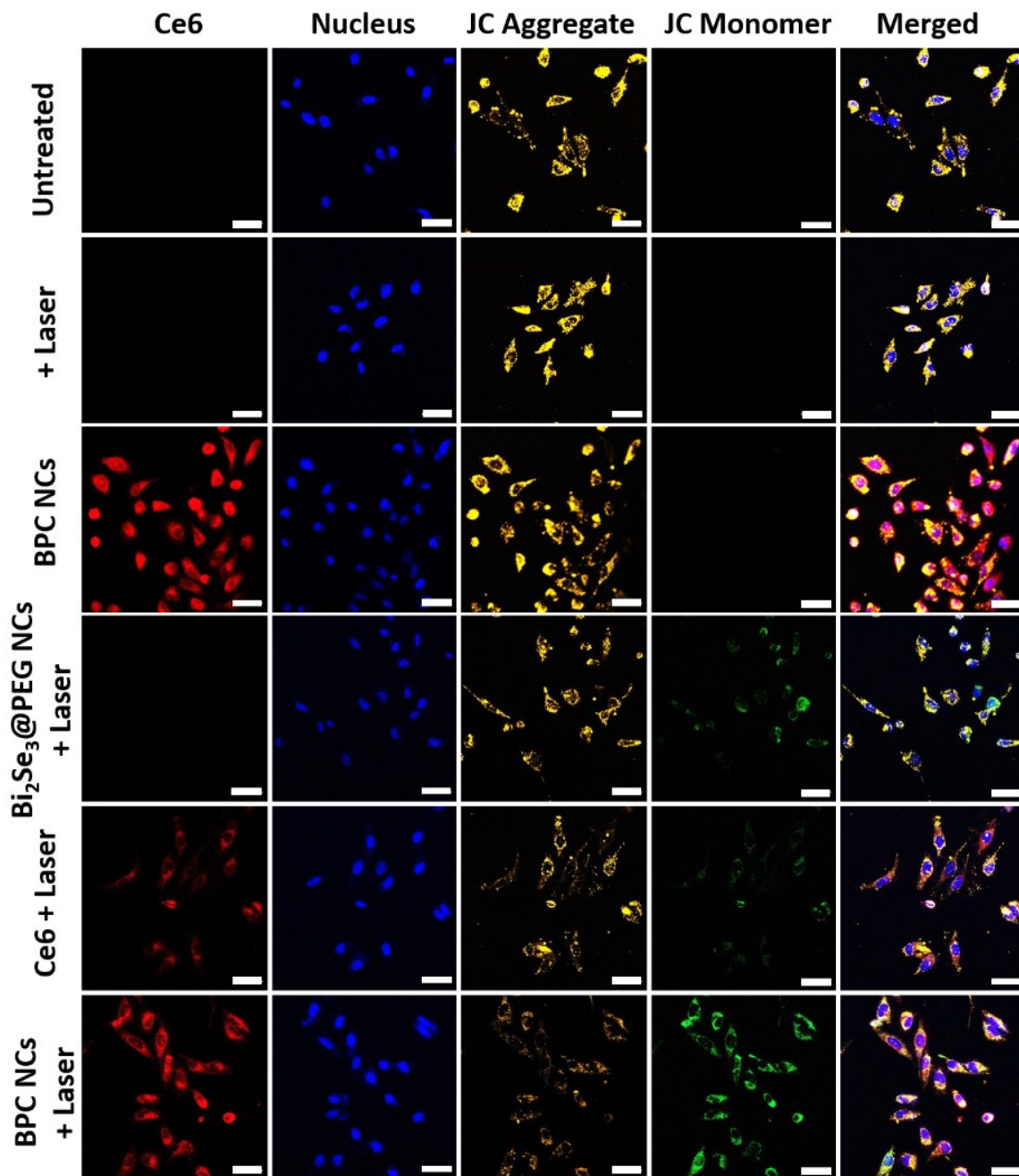


Fig. S13 Fluorescence images of JC-1-labeled HeLa cells after incubation with Bi₂Se₃ NCs, free Ce6 or BPC NCs subject to laser irradiation (660 nm and 808 nm) where applicable (scale bars: 50 μ m).

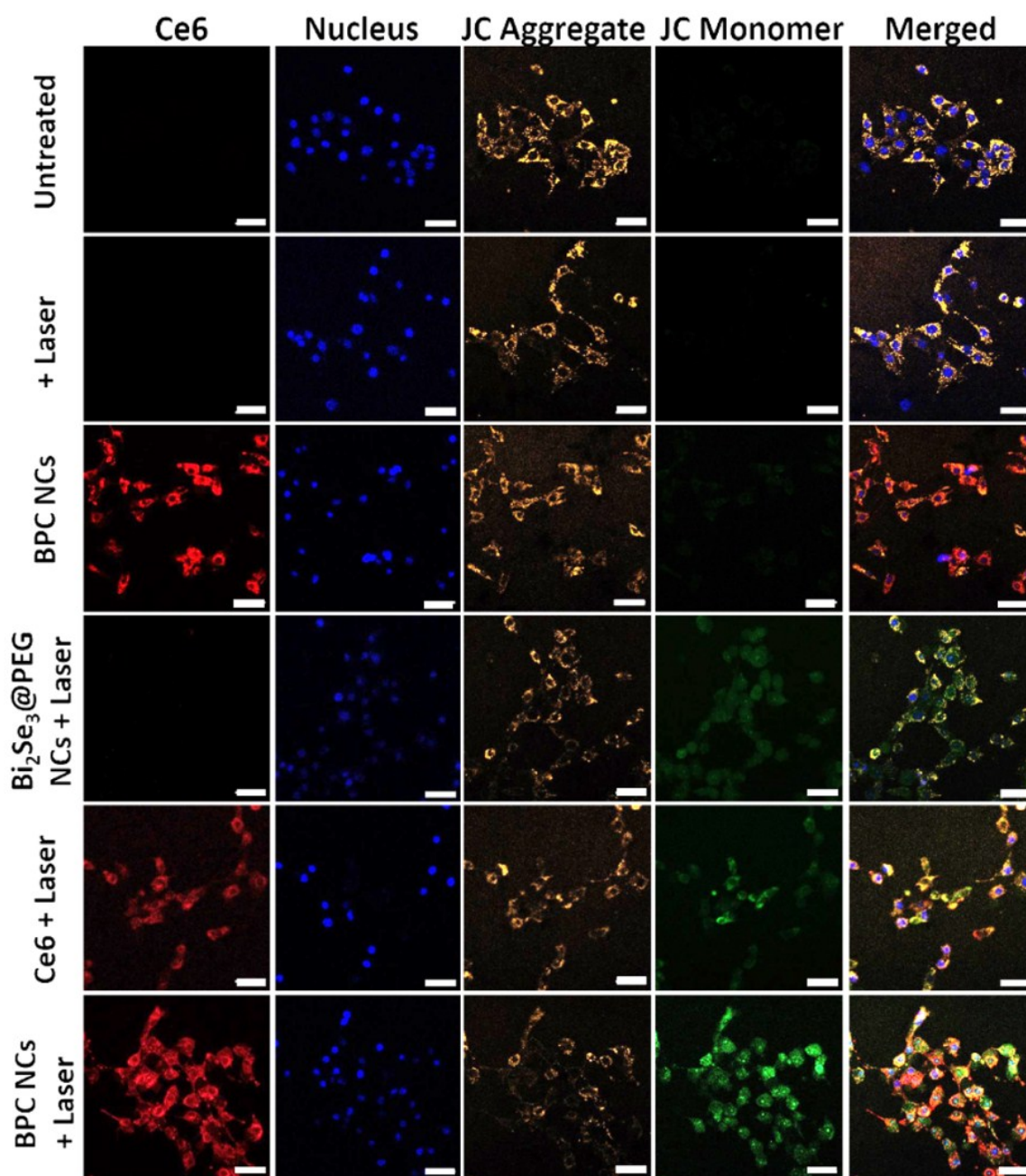


Fig. S14 Fluorescence images of JC-1-labeled 4T1 cells after incubation with Bi₂Se₃ NCs, free Ce6 or BPC NCs subject to laser irradiation (660 nm and 808 nm) where applicable (scale bars: 50 μm).

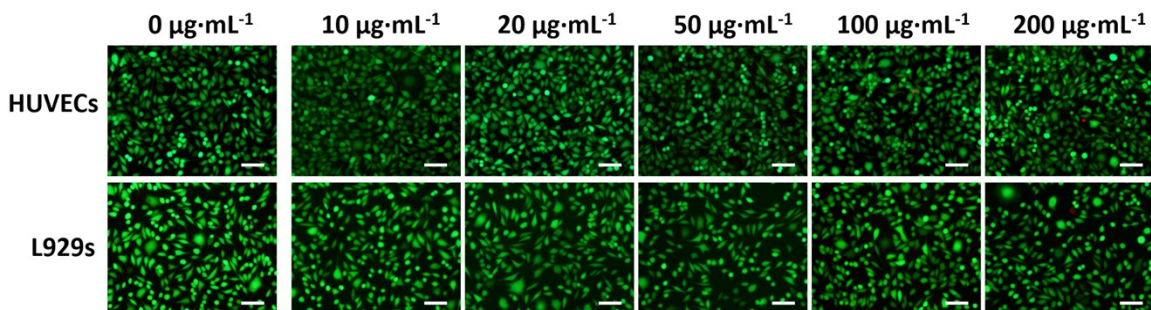


Fig. S15 Fluorescence images to exhibit the viability of HUVECs or L929 cells through LIVE/DEAD viability/cytotoxicity assay kit after cells being treated with different concentrations of $\text{Bi}_2\text{Se}_3@PEG$ NCs for 24h. Live cells were stained with green fluorescence while dead cells were stained with red fluorescence (scale bar: 100 μm).

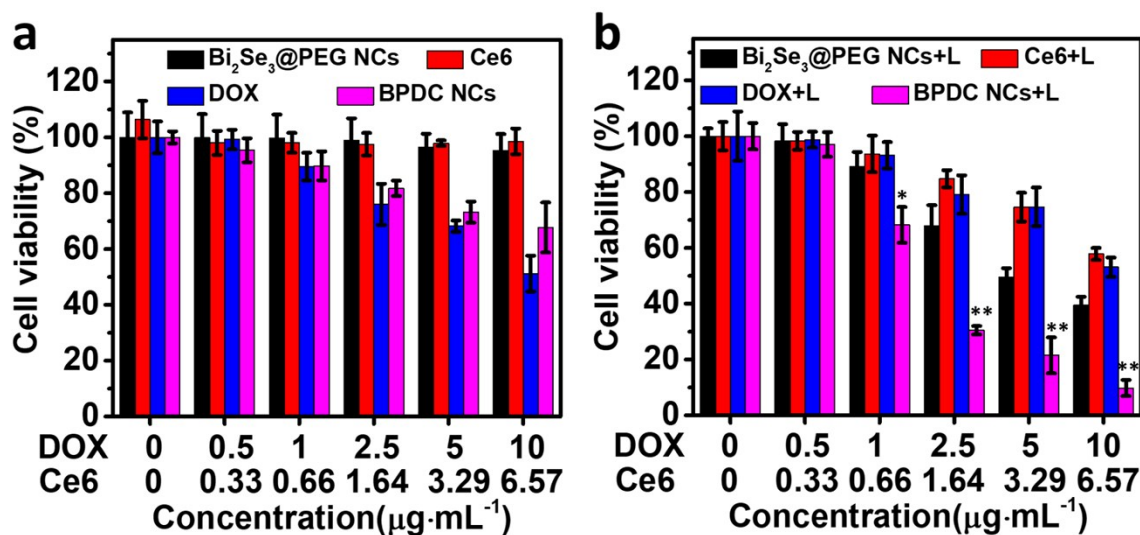


Fig. S16 Viability of 4T1 cells after treatment by $\text{Bi}_2\text{Se}_3@PEG$ NCs, free Ce6, DOX or BPDC NCs (c) with or (d) without laser irradiation (660 nm+808 nm). * $p < 0.05$ and ** $p < 0.01$ when compared to control groups.

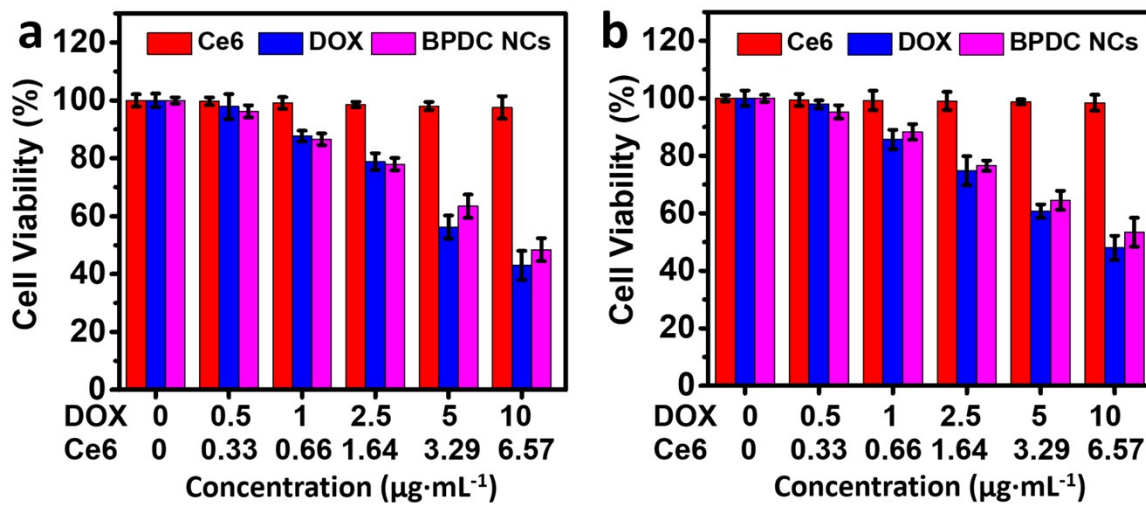


Fig. S17 Dark toxicity of Ce6, DOX and BPDC NCs toward (a) HUVECs and (b) L929s upon the incubation for 24 h in the absence of laser irradiation.

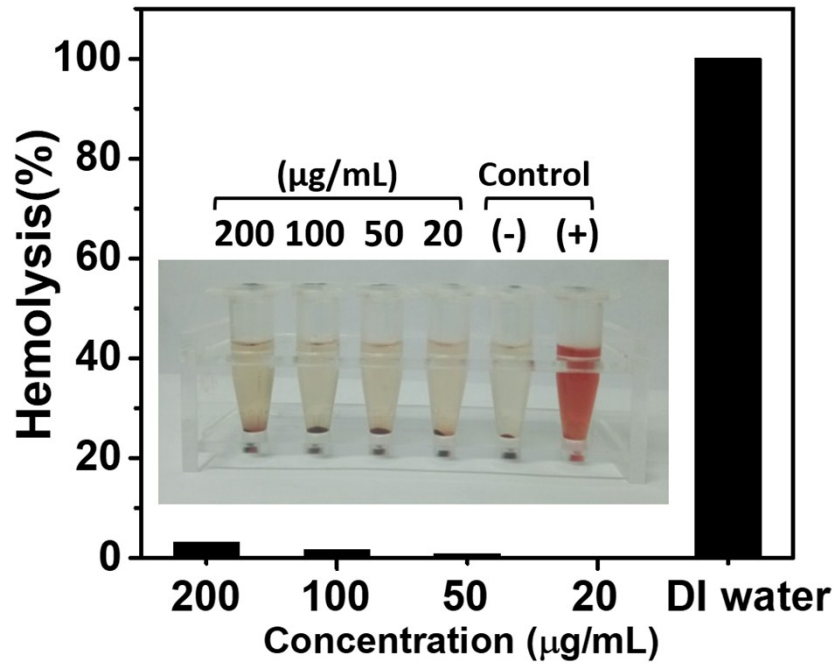


Fig. S18 Hemolysis tests by incubating RBCs with $\text{Bi}_2\text{Se}_3@\text{PEG}$ NCs under various concentrations. Control (+) and Control (-) represent the RBCs in DI water and $1\times\text{PBS}$, respectively.

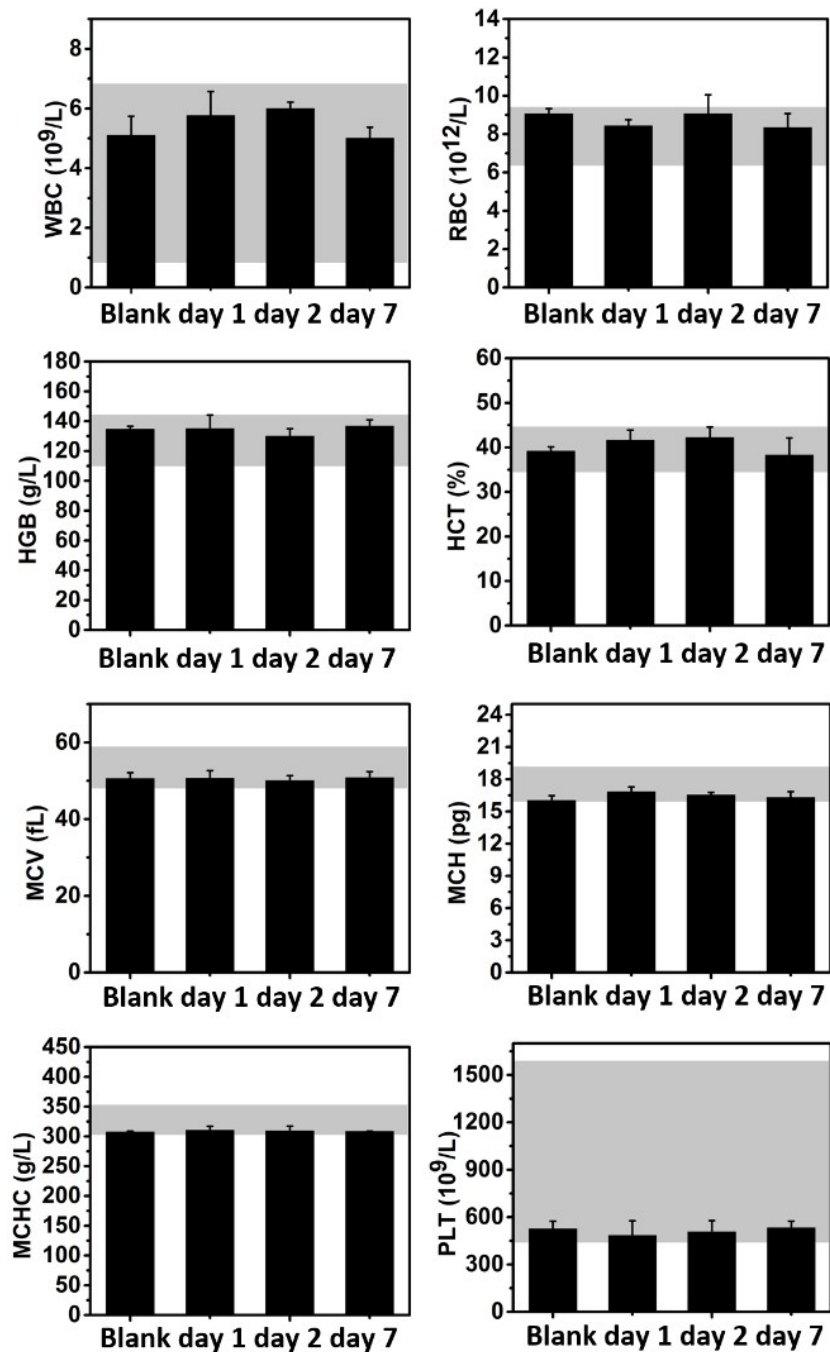


Fig. S19 Primary indicators of blood routine test after KM mice being injected with BPDC NCs. The grey hatched areas represent the reference ranges of hematology data of healthy female KM mice.

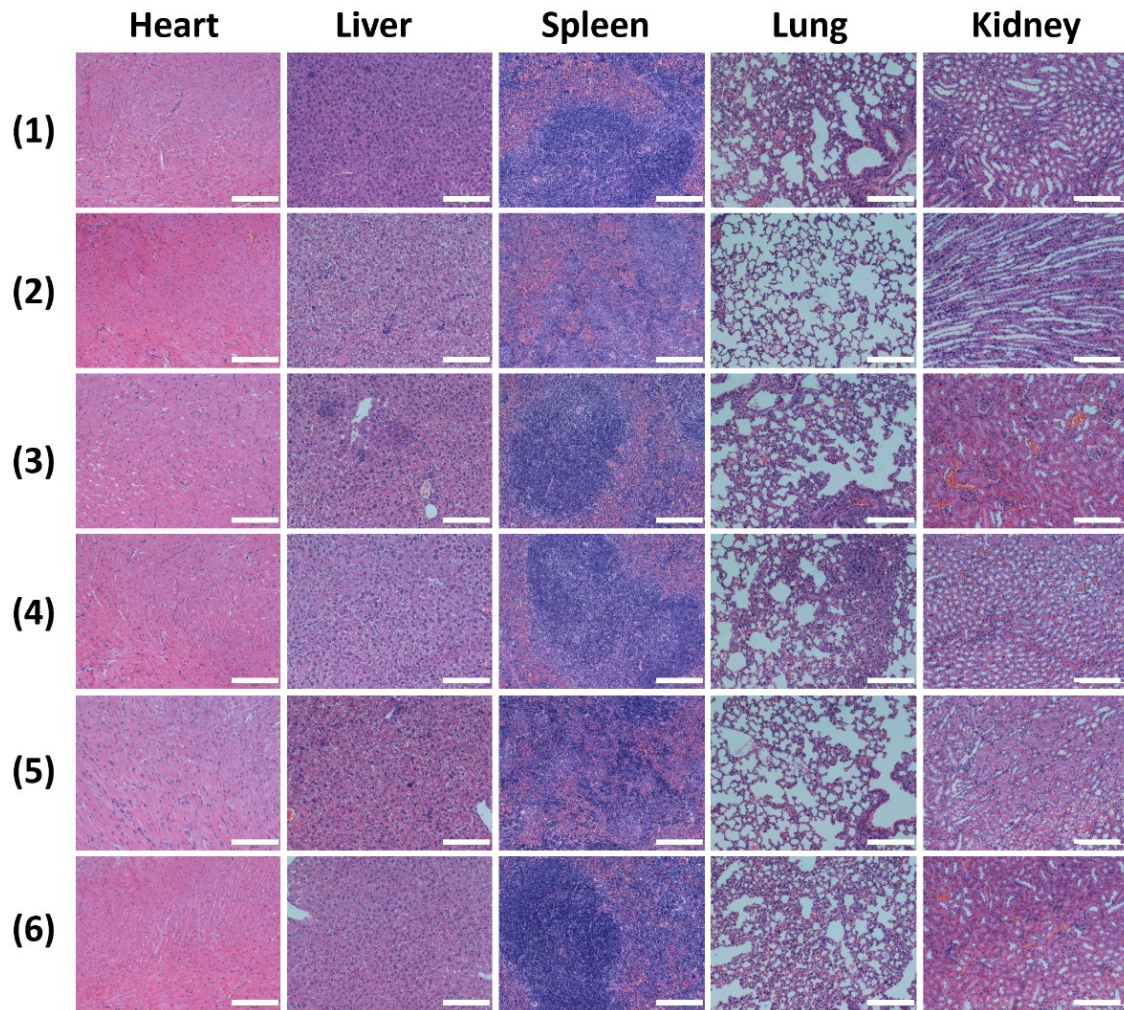


Fig. S20 H&E stained tumor slices from major organs excised from the groups subject to various treatments (scale bars: 100 μm).

Table S1 Complete indicators of blood examinations after mice were injected with BPDC NCs for 7 days.

	<i>Control</i>	<i>1st day</i>	<i>2nd day</i>	<i>7th day</i>	<i>Reference range</i>
WBC (10 ⁹ /L)	5.1±0.63	5.77±0.8	6±0.22	5±0.37	0.8-6.8
Lymph (10 ⁹ /L)	1.13±0.49	2.8±1.01	2.9±0.54	1.63±1.0	0.7-5.7
Mon (10 ⁹ /L)	0.07±0.09	0.16±0.12	0.2±0.16	0.17±0.12	0.0-0.3
Gran (10 ⁹ /L)	1.09±0.24	1.63±0.19	1.7±0.14	1.7±0.75	0.1-1.8
RBC (10 ¹² /L)	9.06±0.27	8.43±0.32	9.06±0.99	8.34±0.73	6.36-9.42
HGB (g/L)	134.7±2.058	135±9.09	130±4.97	133.3±3.83	110-143
HCT (%)	39.17±0.98	41.57±2.32	42.23±2.31	38.3±3.83	34.6-44.6
MCV(fL)	50.57±1.53	50.57±1.95	50.03±1.3	50.8±1.58	48.2-58.3
MCH (pg)	16.03±0.45	16.83±0.45	16.53±0.25	16.3±0.54	15.8-19
MCHC (g/L)	307.67±1.25	310.3±6.6	309±8.29	308.33±0.47	302-353
RDW (%)	16.13±0.59	16.13±0.50	16.1±0.37	16.7±0.16	13-17
PLT (10 ⁹ /L)	526±47.81	483.3±93.67	506.3±72.02	531.3±42.59	450-1590
MPV(fL)	5.5±0.08	4.97±0.78	5.3±0.08	5.47±0.05	3.8-6
PDW	16.67±0.09	16.43±0.37	16.075±0.14	16.47±0.12	
PCT (%)	0.18±0.02	0.24±0.09	0.23±0.03	0.16±0.02	

Calculation of the photothermal conversion efficiency of BPDC NCs¹

The photothermal conversion efficiency (η) of BPDC NCs can be determined following a previously reported method¹. The detailed calculation is provided as follows.

$$\eta = \frac{hS(T_{max} - T_{Surr}) - Q_{Dis}}{I(1 - 10^{-A_{808}})} \quad (1)$$

where h is defined as the heat transfer coefficient, S donates the surface area of the container. The maximum steady temperature (T_{max}) of BPDC NC dispersion is 57.6°C and ambient temperature (T_{Surr}) is 25°C. The laser power I is 2 W, and the absorbance of BPDC NCs at 808 nm is 0.251 (A_{808}). Q_{Dis} represents the heat dissipation from the light source absorbed by the solvent and container, which was measured as 65.52 mW using a quartz cuvette containing DI water.

To calculate hS , a dimensionless parameter θ is defined as

$$\theta = \frac{T - T_{Surr}}{T_{Max} - T_{Surr}} \quad (2)$$

The time constant τ_s of the sample system can be determined as 390.73 seconds based on the fitted curve in Figure S9 according to Equation (3).

$$t = -\tau_s \ln(\theta) \quad (3)$$

The following equation is valid because of energy balance.

$$hS = \frac{m_D C_D}{\tau_s} \quad (4)$$

where m_D denotes the sample mass (1 g) and C_D represents the specific heat of water (4.2 J/g·°C). Then, hS can be calculated as 10.75 mW/°C based on Equation (4). Finally, the photothermal conversion efficiency (η) of BPDC NCs can be calculated as 32.3% by substituting all known parameters in Equation (1).

Reference

1. Tian, Q.; Jiang, F.; Zou, R.; Liu, Q.; Chen, Z.; Zhu, M.; Yang, S.; Wang, J.; Wang, J.; Hu, J. Hydrophilic Cu9S5 Nanocrystals: A Photothermal Agent with a 25.7% Heat Conversion Efficiency for Photothermal Ablation of Cancer Cells in Vivo. *ACS Nano* **2011**, *5*, 9761-9771.